Local-symmetry-sensitive elastic softening in the Kramers doublet system Y$_{1-x}$Nd$_x$Co$_2$Zn$_{20}$

Isao Ishii,[*] Tomohiro Umeno, Rikako Yamamoto, Takahiro Onimaru, and Takashi Suzuki[†]

Department of Quantum Matter, AdSE, Hiroshima University, Higashi-Hiroshima 739-8530, Japan

Koji Araki

Department of Applied Physics, National Defense Academy, Yokosuka, Kanagawa 239-8686, Japan

Atsuhiko Miyata,[‡] Sergei Zherlitsyn, and J. Wosnitza[§]

Hochfeld-Magnetlabor Dresden (HLD-EMFL) and Würzburg-Dresden Cluster of Excellence ct.qmat,
Helmholtz-Zentrum Dresden-Rossendorf, 01328 Dresden, Germany

We investigated the elastic properties of Y$_{1-x}$Nd$_x$Co$_2$Zn$_{20}$ with localized Nd f electrons and ground-state Kramers doublet. All longitudinal and transverse moduli of NdCo$_2$Zn$_{20}$ ($x = 1$) show an elastic softening below 50 K accompanied by a minimum around 2.5 K. The softening, which is robust to magnetic fields up to 8 T, is not observed for samples with Nd concentrations of $x = 0.19$, 0.05, and 0. In localized f electron systems, elastic softening from high temperatures is often understood by crystal electric field effects; however, this cannot explain the behavior in NdCo$_2$Zn$_{20}$. Our experimental and calculated results reveal that the softening neither is caused by a phonon contribution, a Nd^{3+} single-site effect, nor a magnetic interaction. We conclude that the softening is due to a local-symmetry-sensitive electronic state in NdCo$_2$Zn$_{20}$.

I. INTRODUCTION

In the past decade, the Pr-based compounds PrT_2Zn$_{20}$ (T stands for a transition metal) with cubic CeCr$_2$Al$_{20}$-type structure (space group $Fd\bar{3}m$) have attracted much attention due to their fascinating physical properties, such as multipolar ordering, superconductivity, and two-channel Kondo effect [1–15]. Recently, the isostructural NdT_2Zn$_{20}$ series has been studied as well in terms of magnetic ordering, two-channel Kondo effect, and other fascinating properties [16–21].

In this paper, we report on the elastic properties of Nd-based NdCo$_2$Zn$_{20}$ investigated by means of ultrasonic measurements. The cubic lattice parameter of $a = 14.11$ Å is the smallest among the NdT_2Zn$_{20}$ series [18]. The electrical resistivity shows metallic behavior. NdCo$_2$Zn$_{20}$ undergoes an antiferromagnetic ordering at $T_N = 0.53$ K, indicated by a cusp-type anomaly of the magnetic susceptibility in a magnetic field of 0.1 T applied along [100]. Magnetic entropy of $0.5 \times R\ln2$ is released at T_N and it reaches $R\ln2$ at around 4 K, where R is the gas constant.

The magnetic susceptibility follows a Curie-Weiss law from 10 to 300 K. The effective magnetic moment was determined to be $3.90\mu_B$, which is close to the value of $3.62\mu_B$ for the free Nd^{3+}. NdCo$_2$Zn$_{20}$ possesses localized f electrons down to low temperatures. The Nd^{3+} tenfold multiplet with the total angular momentum $J = 9/2$ splits into one Kramers Γ_6 doublet and two Γ_8 quartets by the cubic crystal electric field (CEF), where Γ_i is the irreducible representation. Inelastic neutron scattering experiment revealed that the CEF-level scheme consists of a ground-state Γ_6 Kramers doublet, a first excited Γ_8 quartet at 44 K, and a second excited Γ_8 quartet at 84 K [21]. A Schottky contribution to the specific heat, centered around 13 K, was reproduced by a similar CEF-level scheme [18].

In our previous ultrasonic measurements on NdCo$_2$Zn$_{20}$, we detected an elastic softening of the transverse modulus, C_{44}, below 40 K that continues down to 4.2 K [22]. In localized f electron systems such a characteristic softening of the transverse modulus is a result of a quadrupole-mediated interaction in the CEF [23–32]. The ground-state Γ_6 Kramers doublet has no quadrupole degeneracy. The softening of C_{44}, therefore, may arise from an interlevel quadrupole-mediated interaction between the ground-state doublet and the excited quartets. However, since the first excited quartet exists at 44 K, no elastic softening is expected at low temperatures within the CEF model [22].

In the present study, aiming at understanding the origin of the softening in NdCo$_2$Zn$_{20}$, we measured the longitudinal and transverse elastic moduli using the ultrasonic technique at zero and in applied magnetic fields. In addition, we measured the elastic moduli of the Nd-deficient Y$_{1-x}$Nd$_x$Co$_2$Zn$_{20}$, where YCo$_2$Zn$_{20}$ ($x = 0$) is a nonmagnetic counterpart without f electrons and any phase transition.

---

[*]ish@hiroshima-u.ac.jp

[†]tsuzuki@hiroshima-u.ac.jp

[‡]Present address: Institute for Solid State Physics, University of Tokyo, Kashiwa, Chiba 277-8581, Japan.

[§]Also at Institut für Festkörper- und Materialphysik, TU Dresden, Dresden 01062, Germany.

TABLE I. ρ (g/cm^3) and v (m/s) at 150 K for each measured mode in Y$_{1-x}$Nd$_x$Co$_2$Zn$_{20}$. Measurement errors for v are less than 1%.

x	ρ	v [C_{11}]	v [C_{44}]	v [$(C_{11} - C_{12})/2$]
1	7.424	4279	2695	2536
0.19	7.308	4413	2756	2657
0.05	7.288	4380	2782	2672
0	7.279	4443	2791	2670

II. EXPERIMENTAL DETAILS

Single crystals of Y$_{1-x}$Nd$_x$Co$_2$Zn$_{20}$ were grown by a Zn self-flux method [18]. The composition ratios of the measured samples are $x = 1$, 0.19, 0.05, and 0. Nd concentration x was determined by the results of electron probe microanalysis. The elastic moduli C_{11}, C_{44}, and $(C_{11} - C_{12})/2$ were measured as a function of temperature from 0.3 to 150 K using a phase-comparison pulse-echo method and orthogonal phase-detection technique [33,34]. The modulus C_{11} is related to the longitudinal acoustic mode with $\boldsymbol{k} \parallel \boldsymbol{u} \parallel [001]$, where $\boldsymbol{k}$ and $\boldsymbol{u}$ are the propagation and displacement directions of the ultrasound, respectively. The transverse moduli C_{44} and $(C_{11} - C_{12})/2$ were measured using ($\boldsymbol{k} \parallel [001]$, $\boldsymbol{u} \parallel [110]$) and ($\boldsymbol{k} \parallel [110]$, $\boldsymbol{u} \parallel [1\bar{1}0]$) configurations, respectively. The elastic modulus, C, was calculated from the equation $C = \rho v^2$, with the room-temperature mass density ρ and the measured sound velocity v. The absolute value of the sound velocity was determined at 150 K for each mode using the sample lengths and the time interval between pulse echoes. ρ and v for each x are listed in Table I.

We used LiNbO$_3$ transducers with a fundamental resonance frequency of about 30 MHz. A pair of transducers were glued on the sample surfaces with room-temperature vulcanizing silicone. The magnetic field was applied along [001] using a superconducting magnet.

III. RESULTS AND DISCUSSION

A. Elastic modulus of NdCo$_2$Zn$_{20}$ ($x = 1$)

Figure 1 shows the temperature dependence of the longitudinal elastic modulus C_{11} and the transverse moduli C_{44} and $(C_{11} - C_{12})/2$ in NdCo$_2$Zn$_{20}$. Below 150 K, all moduli first increase monotonically as the temperature decreases. Then, we observe an elastic softening below 45 K in C_{11}, below 30 K in C_{44}, and below 50 K in $(C_{11} - C_{12})/2$. In the insets of Fig. 1, all moduli show an obvious minimum around 2.5 K, which is not related to a phase transition. The minimum as well is not a precursor of the antiferromagnetic ordering because its temperature is substantially higher than T_N. The magnitude of the softening is 1.5, 1.4, and 3.6% in C_{11}, C_{44}, and $(C_{11} - C_{12})/2$, respectively. Although the softening of $(C_{11} - C_{12})/2$ is the largest, other moduli show a considerable softening, suggesting weak anisotropy for symmetry of the strains: ε_{xx}, ε_{yx}, and $\varepsilon_{xx} - \varepsilon_{yy}$, which are corresponding to the C_{11}, C_{44}, and $(C_{11} - C_{12})/2$ modes, respectively. At T_N, all moduli exhibit a steplike softening, reflecting the antiferromagnetic ordering.

We checked whether these softenings are explicable by the known CEF energy-level scheme. For the CEF fits, we
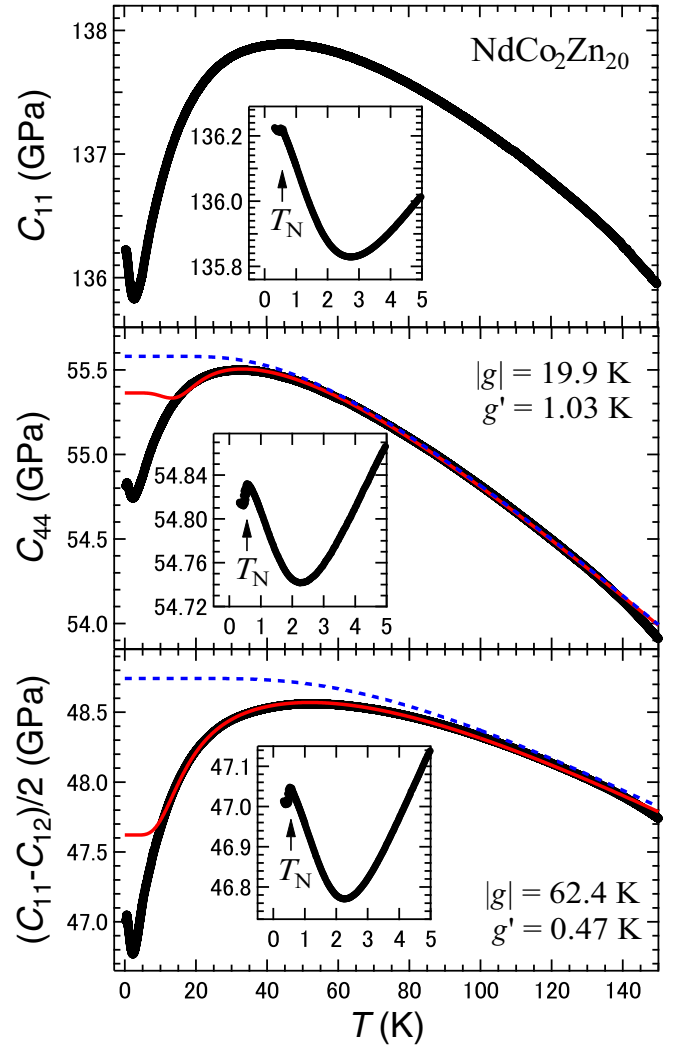

FIG. 1. Temperature dependence of the longitudinal elastic modulus C_{11} (upper panel) as well as the transverse moduli C_{44} (middle panel) and $(C_{11} - C_{12})/2$ (lower panel) of NdCo$_2$Zn$_{20}$ ($x = 1$). The insets display the same data on an expanded temperature scale below 5 K. The red solid and blue dashed lines represent the fit result and the background stiffness, respectively, calculated using the CEF model as discussed in the text. (Notice: from our careful new ultrasonic measurements, we corrected the absolute value of the sound velocity in C_{44} from the data previously reported [22].)

considered the effective Hamiltonian H_{eff}:

$$H_{\mathrm{eff}} = H_{\mathrm{CEF}} - g_i O_i \varepsilon_i - g_i' \langle O_i \rangle O_i,$$

$$H_{\mathrm{CEF}} = W \left[\frac{y}{60} (O_4^0 + 5O_4^4) + \frac{1 - |y|}{1260} (O_6^0 - 21O_6^4) \right],$$

where ε_i, g_i, g_i', W, and O_m^n are the strain, the strain-quadrupole coupling constant, the quadrupole-quadrupole coupling constant, a scale factor of the CEF energy level, and the Stevens equivalent operators, respectively [35,36]. $\langle O_i \rangle$ represents the thermal average of the quadrupole operator, O_i. C_{44} and $(C_{11} - C_{12})/2$ are the linear responses to the ε_{yz} (ε_{zx}, ε_{xy}) and $\varepsilon_{xx} - \varepsilon_{yy}$ [$(2\varepsilon_{zz} - \varepsilon_{xx} - \varepsilon_{yy})/\sqrt{3}$] strains, which couple to the electric quadrupoles O_{yz} (O_{zx}, O_{xy}) and O_2^2 (O_2^0), respectively, in the cubic symmetry. The temperature

TABLE II. Fit parameters of the elastic moduli: $|g_i|$ (K), g_i' (K), C_{0K} (GPa), s (GPa), and t (K) used in the CEF model.

	$|g_i|$	g_i'	C_{0K}	s	t
C_{44}	19.9	1.03	55.6	3.02	160
$(C_{11} - C_{12})/2$	62.4	0.47	48.7	3.34	230

dependence of the elastic modulus, $C(T)$, is calculated using the following equation:

$$C(T) = C_0 \left[\frac{1 - (N_0 g_i^2/C_0 + g_i')\chi_s(T)}{1 - g_i'\chi_s(T)} \right],$$

$$C_0(T) = C_{0K} - \frac{s}{\exp(t/T) - 1},$$

where N_0 ($= 2.848 \times 10^{27}$ m^{-3}) is the number of Nd ions per unit volume at room temperature. χ_s is the quadrupolar (strain) susceptibility for the electric quadrupole moment, as the magnetic susceptibility is the susceptibility for the magnetic dipole moment [37,38]. We adopted the Varshni equation for the background stiffness, $C_0(T)$, with the elastic modulus at 0 K, C_{0K}, and fit parameters, s and t [39].

The red solid lines in Fig. 1 are the fit results using $y = -0.249$ and $W = 0.888$ K obtained by inelastic neutron scattering [21]. Other fit parameters are listed in Table II. The experimental data of C_{44} and $(C_{11} - C_{12})/2$ are well described down to about 15 and 10 K, respectively. However, below these temperatures strong deviations between fit and experiment appear since the interlevel quadrupole-mediated interactions between the ground-state doublet and the first excited quartet at 44 K die out in the low-temperature range. If, hypothetically, the energy splitting between the ground-state doublet and the first excited quartet would be smaller than 10 K or if the ground state would be a Γ_8 quartet, these softenings would be explicable. In these cases, however, the CEF states are inconsistent with the mentioned results obtained from specific-heat and inelastic neutron scattering experiments [18,21]. Consequently, we conclude that the simple CEF model cannot explain the strong softening appearing down to 2.5 K in NdCo$_2$Zn$_{20}$.

B. Elastic modulus of NdCo$_2$Zn$_{20}$ ($x = 1$) under magnetic fields

For further investigating these softenings, we measured all moduli of NdCo$_2$Zn$_{20}$ in magnetic fields of 4 and 8 T applied along [001] (Fig. 2). The softening of the moduli is magnetically robust, hardly changing in magnetic fields. The temperature of the minimum increases only marginally with field in all moduli.

We calculated the transverse moduli for magnetic fields along [001] using the CEF model with the parameters from Sec. III A. The obtained softening is enhanced as the field increases for calculated C_{44} in contrast to calculated $(C_{11} - C_{12})/2$, of which the softening is reduced in magnetic field (not shown), being still largely different from the experimental data.

The authors of Ref. [21] suggested a CEF-phonon bound state and magnetoelastic coupling. In this case, however, considerable magnetic-field and ultrasonic-mode dependences of
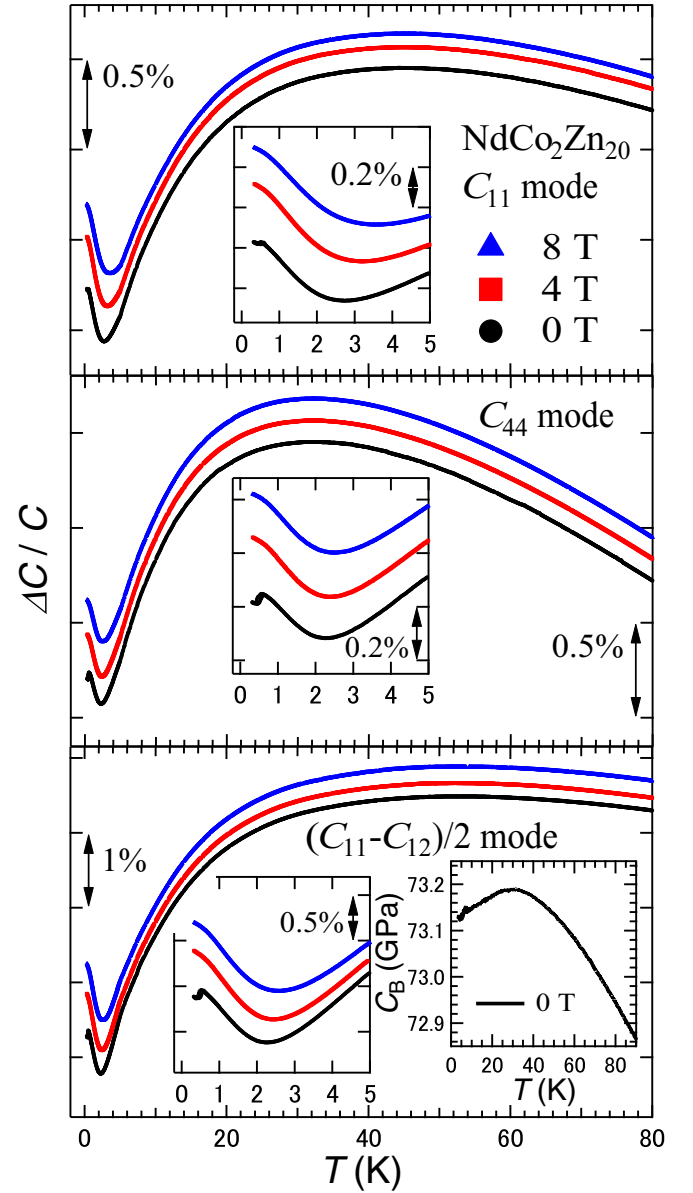

FIG. 2. Temperature dependence of the longitudinal elastic modulus C_{11} (upper panel) as well as the transverse moduli C_{44} (middle panel) and $(C_{11} - C_{12})/2$ (lower panel) in magnetic fields of 4 and 8 T applied along [001] in NdCo$_2$Zn$_{20}$ ($x = 1$). We plotted the moduli as relative change $\Delta C/C$. The data in $H = 4$ and 8 T are vertically offset for clarity. The insets represent the data on an expanded temperature scale below 5 K. The right inset in the lower panel shows the bulk modulus C_B determined for zero magnetic field.

the softening are expected, such as observed in CeAl$_2$ [40]. This contradicts the field- and mode-independent softening observed here.

As another cause for the unusual lattice softening, we examined the possible formation of a heavy-fermion state (a many body effect). This was motivated by the discussion of a possible two-channel Kondo effect in NdCo$_2$Zn$_{20}$ [21]. In a heavy-fermion state, an elastic softening of the bulk modulus, $C_B = (C_{11} + 2C_{12})/3$, which couples to the total-symmetric bulk strain, may occur due to a

deformation-potential coupling. Thereby, the longitudinal modulus, related to the volume-change strain, may exhibit a softening as observed, for instance, in the heavy-fermion compound CeCu$_6$ [41]. However, there is no indication that NdCo$_2$Zn$_{20}$ displays a heavy-fermion state. C_B estimated by using the data of C_{11} and $(C_{11} - C_{12})/2$ shows a very slight softening below 30 K (the right inset in the lower panel in Fig. 2). However, this softening is less than 0.1%, which is considerably smaller than the softening of the other moduli. The transverse moduli exhibit a softening down to the same temperature as the minimum of C_{11}. In addition, the softening in the elastic moduli remains robust even in the presence of magnetic fields, whereas, generally, the Kondo effect is expected to collapse in a magnetic field. Hence the softening observed in NdCo$_2$Zn$_{20}$ cannot be attributed to the formation of a heavy-fermion state.

C. Elastic modulus of Nd-deficient Y$_{1-x}$Nd$_x$Co$_2$Zn$_{20}$

To investigate whether the softening arises from the $4f$ electrons of Nd^{3+} or from a phonon contribution, we conducted ultrasonic measurements of Y$_{1-x}$Nd$_x$Co$_2$Zn$_{20}$ with small Nd concentrations of $x = 0.19$, 0.05, and 0. The temperature dependences of the elastic moduli C_{11}, C_{44}, and $(C_{11} - C_{12})/2$ are shown in Fig. 3. Contrary to the softening observed in NdCo$_2$Zn$_{20}$, the Nd-deficient samples show no obvious elastic softening down to 1.8 K for C_{11} and C_{44} and down to 0.3 K for $(C_{11} - C_{12})/2$. This absence of elastic softening in YCo$_2$Zn$_{20}$ ($x = 0$) evidences that the softening is not ascribed to the phonon contribution and that the $4f$ electrons of Nd^{3+} play a crucial role.

If the elastic softening would originate from a Nd^{3+} single-site effect, such as a CEF effect, one would expect that this softening occurs even in the $x = 0.19$ and 0.05 samples. The magnitude of the softening would then scale with the Nd concentration x. However, the Nd-deficient samples exhibit no softening down to 0.3 K at all. Therefore, the softening is not caused by a Nd^{3+} single-site effect. Consequently, the presence of the Nd network in the diamond sublattice must lead to the emergence of degrees of freedom that causes the softening.

Further, in preliminary ultrasonic measurements of the isomorphic compound NdRh$_2$Zn$_{20}$, we found no evident softening in any of the elastic moduli down to 4.2 K (not shown). NdRh$_2$Zn$_{20}$ undergoes a first-order structural transition around 240 K [18], indicating that the symmetry of the crystal structure is lowered, which seems to quench the degrees of freedom that cause the softening. To put it in another way, the high symmetry of the cubic structure is necessary for the softening in NdCo$_2$Zn$_{20}$.

The above considerations evidence that the localized $4f$ electrons of Nd^{3+} in the high symmetric cubic structure are crucial. Here, it is noted that the CEF excitation peak observed at 3.8 meV by means of inelastic neutron scattering is broader than those observed in NdRh$_2$Zn$_{20}$ and NdIr$_2$Zn$_{20}$ [21]. The broadening of the CEF excitation peak may be attributed to fluctuations that result from many-body correlations. We discuss a possible many-body electronic state, which is significantly affected by the substituted nonmagnetic yttrium ions, in the next subsection.
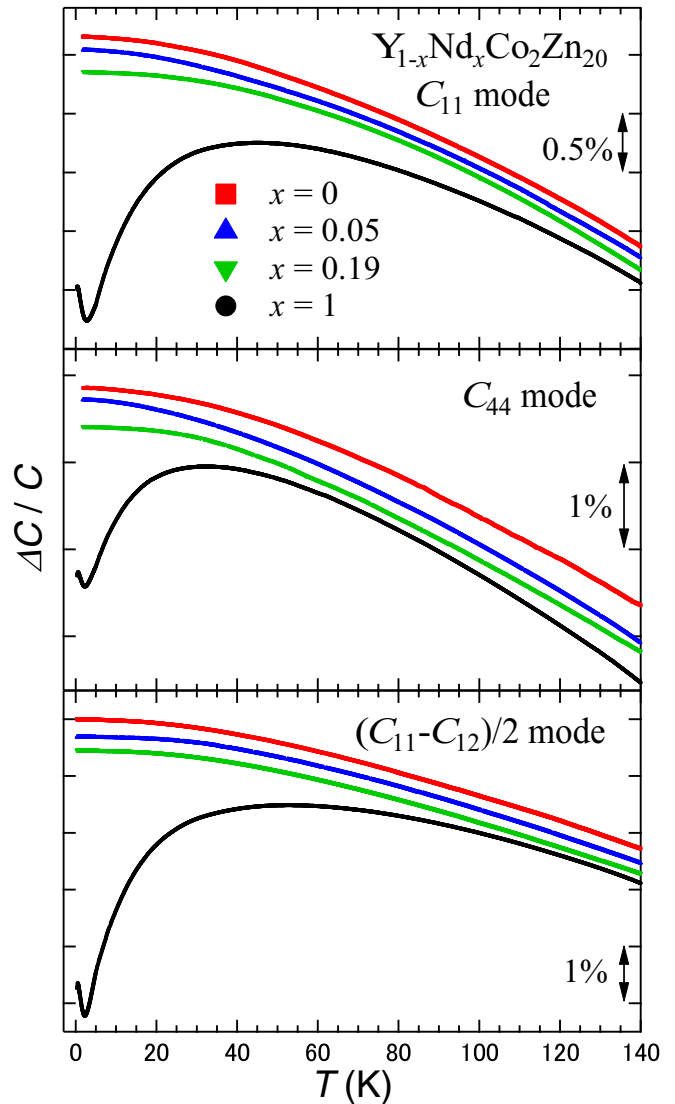

FIG. 3. Temperature dependence of the longitudinal elastic modulus C_{11} (upper panel) as well as the transverse moduli C_{44} (middle panel) and $(C_{11} - C_{12})/2$ (lower panel) for Y$_{1-x}$Nd$_x$Co$_2$Zn$_{20}$ ($x = 1$, 0.19, 0.05, and 0). The data are shifted along the vertical axis for clarity.

D. Many-body electronic state

NdCo$_2$Zn$_{20}$ shows a magnetically robust lattice softening from high temperatures with a sharp minimum without any phase transition. This elastic behavior is similar to that arising from two splitted energy states. The elastic modulus in such a case was discussed for two-dimensional dimer systems such as SrCu$_2$(BO$_3$)$_2$, spinel systems, and caged compounds [42–49]. We can describe the elastic moduli qualitatively using two energy states using a small level spacing of ∼3.5 K (not shown). This level spacing is much smaller than the CEF energy splitting determined by inelastic neutron scattering [21]. To date, no other experiment evidences an anomaly at this low energy scale [18].

Despite this, we explore the potential of this scenario. The ground-state Γ_6 doublet, isolated from the first excited Γ_8 quartet at 44 K, has only spin degrees of freedom at

sufficiently low temperatures. However, there are no reports on the formation of a spin multimer or a low-dimensional magnetic state in $NdCo_2Zn_{20}$, in contrast to the mentioned cases of $SrCu_2(BO_3)_2$ and spinel compounds [18,42–47,50]. In fact, the magnetic susceptibility shows no anomaly above T_N in $NdCo_2Zn_{20}$. These results and the magnetically robust elastic softening suggest that the many-body electronic state cannot be caused by magnetic interactions.

For caged compounds, a large-amplitude atomic motion of a guest atom, called rattling motion, was reported in the isomorphic compounds LaT_2Zn_{20} [1,51–53]. The Zn ion at the 16c site sits in a polyhedral cage consisting of two rare-earth ions and twelve Zn ions at the 96g site. It was reported that the Zn ion at the 16c site oscillates perpendicular to the La-Zn(16c)-La connection line [53]. The isomorphic compounds PrT_2Zn_{20} exhibit an ultrasonic dispersion, seen in the ultrasonic frequency dependence of an elastic modulus and ultrasonic attenuation. Ultrasonic dispersion is a characteristic behavior of the rattling motion [6,10,26,54]. In $NdCo_2Zn_{20}$, however, no rattling motion was reported. Furthermore, in our experimental results, ultrasonic dispersion is not detected and the reference compound YCo_2Zn_{20} ($x = 0$) shows no elastic softening (Fig. 3).

From another perspective, a Nd^{3+} is placed in a Frank-Kasper cage consisting of sixteen Zn ions [3]. If these ions form a cluster, there exists the possibility that a molecularlike many-body electronic state is formed by mixing the J multiplet of Nd^{3+} with the ligand p electrons of the Zn ions. The many-body electronic state may possess fluctuations. In such a case, a broadening of the CEF excitation peaks observed in inelastic neutron scattering is expected. The fluctuations may couple to phonons giving rise to elastic softening due to a lattice instability. Because the high symmetry of the cubic structure is crucial for the softening in $NdCo_2Zn_{20}$, as discussed in Sec. III C, the many-body electronic state could be easily disturbed by substituting Y^{3+} for Nd^{3+}. Thereby, the elastic softening by the lattice instability vanishes due to the symmetry lowering, which may break the many-body electronic state in the Nd-deficient $Y_{1-x}Nd_xCo_2Zn_{20}$

($x = 0.19$, 0.05, and 0) samples. Indeed, classification of a cluster multipole consisting of several atoms/ions has recently been established [55–57]. As a result, the elastic softening in $NdCo_2Zn_{20}$ might be related to a cluster multipole.

Consequently, in $NdCo_2Zn_{20}$ we have discovered an elastic softening robust in magnetic field. The softening is not caused by a phonon contribution, nor by a Nd^{3+} single-site effect, nor by magnetic interactions. We propose a many-body electronic state between the J multiplet of Nd^{3+} and the ligand electrons as a reason for the softening. However, there are still open questions regarding the driving force behind the many-body electronic state. To answer these questions, further theoretical studies and microscopic experiments are necessary.

IV. CONCLUSION

We performed ultrasonic measurements on $Y_{1-x}Nd_xCo_2Zn_{20}$ for $x = 1$, 0.19, 0.05, and 0. In $NdCo_2Zn_{20}$ ($x = 1$), we observed an elastic softening accompanied by a minimum around 2.5 K in all moduli. We revealed that the softening is insensitive to magnetic field. A simple CEF model cannot explain the lattice softening. We found no softening in the samples with $x = 0.19$, 0.05, and 0, suggesting no contribution of phonon and single-site effects of Nd^{3+}. We suggest a possible formation of a many-body electronic state through the correlation between the J multiplet of Nd^{3+} and ligand electrons.

[1] T. Nasch, W. Jeitschko, and U. C. Rodewald, Ternary rare earth transition metal zinc compounds RT_2Zn_{20} with $T =$ Fe, Ru, Co, Rh, and Ni, Z. Naturforsch. **52**, 1023 (1997).

[2] S. Jia, N. Ni, S. L. Bud'ko, P. C. Canfield, and G. Lu, Magnetic properties of RFe_2Zn_{20} and RCo_2Zn_{20} ($R =$ Y, Nd, Sm, Gd-Lu), Phys. Rev. B **80**, 104403 (2009).

[3] T. Onimaru and H. Kusunose, Exotic quadrupolar phenomena in non-Kramers doublet systems –the cases of PrT_2Zn_{20} ($T =$ Ir, Rh) and PrT_2Al_{20} ($T =$ V, Ti)–, J. Phys. Soc. Jpn. **85**, 082002 (2016).

[4] T. Onimaru, K. T. Matsumoto, Y. F. Inoue, K. Umeo, Y. Saiga, Y. Matsushita, R. Tamura, K. Nishimoto, I. Ishii, T. Suzuki, and T. Takabatake, Superconductivity and structural phase transitions in caged compounds RT_2Zn_{20} ($R =$ La, Pr, $T =$ Ru, Ir), J. Phys. Soc. Jpn. **79**, 033704 (2010).

[5] T. Onimaru, K. T. Matsumoto, Y. F. Inoue, K. Umeo, T. Sakakibara, Y. Karaki, M. Kubota, and T. Takabatake, Antifer-

roquadrupolar ordering in a Pr-based superconductor $PrIr_2Zn_{20}$, Phys. Rev. Lett. **106**, 177001 (2011).

[6] I. Ishii, H. Muneshige, Y. Suetomi, T. K. Fujita, T. Onimaru, K. T. Matsumoto, T. Takabatake, K. Araki, M. Akatsu, Y. Nemoto, T. Goto, and T. Suzuki, Antiferro-quadrupolar ordering at the lowest temperature and anisotropic magnetic field-temperature phase diagram in the cage compound $PrIr_2Zn_{20}$, J. Phys. Soc. Jpn. **80**, 093601 (2011).

[7] K. Iwasa, K. T. Matsumoto, T. Onimaru, T. Takabatake, J. M. Mignot, and A. Gukasov, Evidence for antiferromagnetic-type ordering of f-electron multipoles in $PrIr_2Zn_{20}$, Phys. Rev. B **95**, 155106 (2017).

[8] K. Umeo, R. Takikawa, T. Onimaru, M. Adachi, K. T. Matsumoto, and T. Takabatake, Simultaneous collapse of antiferroquadrupolar order and superconductivity in $PrIr_2Zn_{20}$ by nonhydrostatic pressure, Phys. Rev. B **102**, 094505 (2020).

[9] T. Onimaru, N. Nagasawa, K. T. Matsumoto, K. Wakiya, K. Umeo, S. Kittaka, T. Sakakibara, Y. Matsushita, and T. Takabatake, Simultaneous superconducting and antiferroquadrupolar transitions in PrRh$_2$Zn$_{20}$, Phys. Rev. B **86**, 184426 (2012).

[10] I. Ishii, H. Muneshige, S. Kamikawa, T. K. Fujita, T. Onimaru, N. Nagasawa, T. Takabatake, T. Suzuki, G. Ano, M. Akatsu, Y. Nemoto, and T. Goto, Antiferroquadrupolar ordering and magnetic-field-induced phase transition in the cage compound PrRh$_2$Zn$_{20}$, Phys. Rev. B **87**, 205106 (2013).

[11] I. Ishii, H. Goto, S. Kamikawa, S. Yasin, S. Zherlitsyn, J. Wosnitza, T. Onimaru, K. T. Matsumoto, T. Takabatake, and T. Suzuki, Exotic ground state and elastic softening under pulsed magnetic fields in PrTr_2Zn$_{20}$ (Tr = Rh, Ir), J. Phys. Soc. Jpn. **85**, 043601 (2016).

[12] D. L. Cox, Quadrupolar Kondo effect in uranium heavy-electron materials? Phys. Rev. Lett. **59**, 1240 (1987).

[13] Y. Yamane, T. Onimaru, K. Wakiya, K. T. Matsumoto, K. Umeo, and T. Takabatake, Single-site non-Fermi-liquid behaviors in a diluted $4f^2$ system Y$_{1-x}$Pr$_x$Ir$_2$Zn$_{20}$, Phys. Rev. Lett. **121**, 077206 (2018).

[14] T. Yanagisawa, H. Hidaka, H. Amitsuka, S. Zherlitsyn, J. Wosnitza, Y. Yamane, and T. Onimaru, Evidence for the single-site quadrupolar Kondo effect in the dilute non-Kramers system Y$_{1-x}$Pr$_x$Ir$_2$Zn$_{20}$, Phys. Rev. Lett. **123**, 067201 (2019).

[15] T. Onimaru, K. Izawa, K. T. Matsumoto, T. Yoshida, Y. Machida, T. Ikeura, K. Wakiya, K. Umeo, S. Kittaka, K. Araki, T. Sakakibara, and T. Takabatake, Quadrupole-driven non-Fermi-liquid and magnetic-field-induced heavy fermion states in a non-Kramers doublet system, Phys. Rev. B **94**, 075134 (2016).

[16] T. Hotta, Two-channel Kondo effect emerging from Nd ions, J. Phys. Soc. Jpn. **86**, 083704 (2017).

[17] Y. Yamane, R. J. Yamada, T. Onimaru, K. Uenishi, K. Wakiya, K. T. Matsumoto, K. Umeo, and T. Takabatake, Competing magnetic interactions in the Kramers doublet system NdIr$_2$Zn$_{20}$, J. Phys. Soc. Jpn. **86**, 054708 (2017).

[18] R. Yamamoto, T. Onimaru, R. J. Yamada, Y. Yamane, Y. Shimura, K. Umeo, and T. Takabatake, Antiferromagnetic order of NdT_2Zn$_{20}$ (T = Co and Rh) with the Kramers Γ_6 doublet ground state, J. Phys. Soc. Jpn. **88**, 044703 (2019).

[19] R. Yamamoto, T. Onimaru, Y. Yamane, Y. Shimura, K. Umeo, and T. Takabatake, Magnetic properties of a diluted Nd system Y$_{1-x}$Nd$_x$Co$_2$Zn$_{20}$ for $x = 0.20$ with a Γ_6 doublet ground state, JPS Conf. Proc. **29**, 015006 (2020).

[20] R. Yamamoto, R. J. Yamada, Y. Yamane, Y. Shimura, K. Umeo, T. Takabatake, and T. Onimaru, Effect of Ga and Cd substitutions on the first-order antiferromagnetic transition in NdCo$_2$Zn$_{20}$, Phys. Rev. B **104**, 155112 (2021).

[21] R. Yamamoto, M. D. Le, D. T. Adroja, Y. Shimura, T. Takabatake, and T. Onimaru, Inelastic neutron scattering study of crystalline electric field excitations, in the caged compounds NdT_2Zn$_{20}$ (T = Co, Rh, and Ir), Phys. Rev. B **107**, 075114 (2023).

[22] T. Umeno, I. Ishii, S. Kumano, D. Suzuki, R. Yamamoto, T. Onimaru, and T. Suzuki, Crystal electric field response in elastic modulus without rattling effect in the cage compound NdCo$_2$Zn$_{20}$, JPS Conf. Proc. **30**, 011162 (2020).

[23] T. Suzuki, I. Ishii, N. Okuda, K. Katoh, T. Takabatake, T. Fujita, and A. Tamaki, Quadrupolar ordering of $5f$ electrons in UCu$_2$Sn, Phys. Rev. B **62**, 49 (2000).

[24] Y. Nakanishi, T. Sakon, M. Motokawa, M. Ozawa, T. Suzuki, and M. Yoshizawa, Elastic properties and phase diagram of the rare-earth monopnictide TbSb, Phys. Rev. B **68**, 144427 (2003).

[25] T. Yanagisawa, T. Goto, Y. Nemoto, S. Miyata, R. Watanuki, and K. Suzuki, Ultrasonic investigation of quadrupole ordering in HoB$_2$C$_2$, Phys. Rev. B **67**, 115129 (2003).

[26] T. Goto, Y. Nemoto, K. Sakai, T. Yamaguchi, M. Akatsu, T. Yanagisawa, H. Hazama, K. Onuki, H. Sugawara, and H. Sato, Quadrupolar effect and rattling motion in the heavy-fermion superconductor PrOs$_4$Sb$_{12}$, Phys. Rev. B **69**, 180511(R) (2004).

[27] I. Ishii, K. Takezawa, T. Mizuno, S. Kamikawa, H. Ninomiya, Y. Matsumoto, S. Ohara, K. Mitsumoto, and T. Suzuki, Ferroquadrupolar ordering due to the quasi-degenerate quartet in the trigonal chiral structure of DyNi$_3$Ga$_9$, J. Phys. Soc. Jpn. **87**, 013602 (2018).

[28] I. Ishii, K. Takezawa, T. Mizuno, S. Kumano, T. Suzuki, H. Ninomiya, K. Mitsumoto, K. Umeo, S. Nakamura, and S. Ohara, Anisotropic phase diagram of ferroquadrupolar ordering in the trigonal chiral compound DyNi$_3$Ga$_9$, Phys. Rev. B **99**, 075156 (2019).

[29] I. Ishii, T. Mizuno, K. Takezawa, S. Kumano, Y. Kawamoto, T. Suzuki, D. I. Gorbunov, M. S. Henriques, and A. V. Andreev, Magnetic-field-induced quadrupolar ordering and the crystal electric field effect in the distorted kagome lattice antiferromagnet Dy$_3$Ru$_4$Al$_{12}$, Phys. Rev. B **97**, 235130 (2018).

[30] D. I. Gorbunov, T. Nomura, I. Ishii, M. S. Henriques, A. V. Andreev, M. Doerr, T. Stöter, T. Suzuki, S. Zherlitsyn, and J. Wosnitza, Crystal-field effects in the kagome antiferromagnet Ho$_3$Ru$_4$Al$_{12}$, Phys. Rev. B **97**, 184412 (2018).

[31] I. Ishii, D. Suzuki, T. Umeno, Y. Kurata, Y. Wada, T. Suzuki, A. V. Andreev, D. I. Gorbunov, A. Miyata, S. Zherlitsyn, and J. Wosnitza, Distinct field-induced ferroquadrupolar states for two different magnetic-field directions in DyNiAl, Phys. Rev. B **103**, 195151 (2021).

[32] I. Ishii, Y. Kurata, Y. Wada, M. Nohara, T. Suzuki, K. Araki, and A. V. Andreev, Ferroquadrupolar ordering in a magnetically ordered state in ErNiAl, Phys. Rev. B **105**, 165147 (2022).

[33] T. J. Moran and B. Lüthi, Elastic and magnetoelastic effects in magnetite, Phys. Rev. **187**, 710 (1969).

[34] B. Wolf, B. Lüthi, S. Schmidt, H. Schwenk, M. Sieling, S. Zherlitsyn, and I. Kouroudis, New experimental techniques for pulsed magnetic fields – ESR and ultrasonics, Phys. B: Condens. Matter **294-295**, 612 (2001).

[35] K. R. Lea, M. J. M. Leask, and W. P. Wolf, The raising of angular momentum degeneracy of f-electron terms by cubic crystal fields, J. Phys. Chem. Solids **23**, 1381 (1962).

[36] M. T. Hutchings, Point-charge calculations of energy levels of magnetic ions in crystalline electric fields, Solid State Phys. **16**, 227 (1964).

[37] B. Lüthi, Interaction of magnetic ions with phonons, in *Dynamical Properties of Solids*, edited by G. K. Horton and A. A. Maradudin (North-Holland, Amsterdam, 1980), Vol. 3, Chap. 4, pp. 245–292.

[38] See Supplemental Material of Ref. [28].

[39] Y. P. Varshni, Temperature dependence of the elastic constants, Phys. Rev. B **2**, 3952 (1970).

[40] B. Lüthi and C. Lingner, Magnetoelasticity, rotational invariance and magnetoacoustic birefringence in CeAl$_2$, Z. Phys. B **34**, 157 (1979).

[41] T. Suzuki, T. Goto, A. Tamaki, T. Fujimura, Y. Ōnuki, and T. Komatsubara, Elastic soft mode and crystalline field effect of Kondo lattice substance; CeCu$_6$, J. Phys. Soc. Jpn. **54**, 2367 (1985).

[42] S. Zherlitsyn, S. Schmidt, B. Wolf, H. Schwenk, B. Lüthi, H. Kageyama, K. Onizuka, Y. Ueda, and K. Ueda, Sound-wave anomalies in SrCu$_2$(BO$_3$)$_2$, Phys. Rev. B **62**, R6097 (2000).

[43] B. Wolf, S. Zherlitsyn, S. Schmidt, B. Lüthi, H. Kageyama, and Y. Ueda, Soft acoustic modes in the two-dimensional spin system SrCu$_2$(BO$_3$)$_2$, Phys. Rev. Lett. **86**, 4847 (2001).

[44] T. Watanabe, S. Hara, S. Ikeda, and K. Tomiyasu, Elastic instabilities in an antiferromagnetically ordered phase of the orbitally frustrated spinel GeCo$_2$O$_4$, Phys. Rev. B **84**, 020409(R) (2011).

[45] T. Watanabe, S. Ishikawa, H. Suzuki, Y. Kousaka, and K. Tomiyasu, Observation of elastic anomalies driven by co-existing dynamical spin Jahn-Teller effect and dynamical molecular-spin state in the paramagnetic phase of frustrated MgCr$_2$O$_4$, Phys. Rev. B **86**, 144413 (2012).

[46] T. Watanabe, T. Ishikawa, S. Hara, A. T. M. Nazmul Islam, E. M. Wheeler, and B. Lake, Multiple lattice instabilities resolved by magnetic-field and disorder sensitivities in MgV$_2$O$_4$, Phys. Rev. B **90**, 100407(R) (2014).

[47] T. Watanabe, S. Takita, K. Tomiyasu, and K. Kamazawa, Acoustic study of dynamical molecular-spin state without magnetic phase transition in spin-frustrated ZnFe$_2$O$_4$, Phys. Rev. B **92**, 174420 (2015).

[48] V. Keppens, D. Mandrus, B. C. Sales, B. C. Chakoumakos, P. Dai, R. Coldea, M. B. Maple, D. A. Gajewski, E. J. Freeman, and S. Bennington, Localized vibrational modes in metallic solids, Nature (London) **395**, 876 (1998).

[49] I. Zerec, V. Keppens, M. A. McGuire, D. Mandrus, B. C. Sales, and P. Thalmeier, Four-well tunneling states and elastic response of clathrates, Phys. Rev. Lett. **92**, 185502 (2004).

[50] H. Kageyama, K. Yoshimura, R. Stern, N. V. Mushnikov, K. Onizuka, M. Kato, K. Kosuge, C. P. Slichter, T. Goto, and Y. Ueda, Exact dimer ground state and quantized magnetization plateaus in the two-dimensional spin system SrCu$_2$(BO$_3$)$_2$, Phys. Rev. Lett. **82**, 3168 (1999).

[51] H. Tou, K. Asaki, H. Kotegawa, T. Onimaru, K. T. Matsumoto, Y. F. Inoue, and T. Takabatake, Evidence of a rattling transition in the caged compounds LaRu$_2$Zn$_{20}$ and LaIr$_2$Zn$_{20}$: ^{139}La NMR studies, J. Korean Phys. Soc. **63**, 650 (2013).

[52] K. Wakiya, T. Onimaru, S. Tsutsui, T. Hasegawa, K. T. Matsumoto, N. Nagasawa, A. Q. R. Baron, N. Ogita, M. Udagawa, and T. Takabatake, Low-energy optical phonon modes in the caged compound LaRu$_2$Zn$_{20}$, Phys. Rev. B **93**, 064105 (2016).

[53] T. Hasegawa, N. Ogita, and M. Udagawa, First-principles calculations of lattice vibrations on LaT_2Zn$_{20}$ (T = Ru and Ir), J. Phys.: Conf. Ser. **391**, 012016 (2012).

[54] I. Ishii, Y. Suetomi, T. K. Fujita, K. Suekuni, T. Tanaka, T. Takabatake, T. Suzuki, and M. A. Avila, Lattice instability and elastic dispersion due to the rattling motion in the type-I clathrate Ba$_8$Ga$_{16}$Sn$_{30}$, Phys. Rev. B **85**, 085101 (2012).

[55] S. Hayami, M. Yatsushiro, Y. Yanagi, and H. Kusunose, Classification of atomic-scale multipoles under crystallographic point groups and application to linear response tensors, Phys. Rev. B **98**, 165110 (2018).

[56] S. Hayami and H. Kusunose, Microscopic description of electric and magnetic toroidal multipoles in hybrid orbitals, J. Phys. Soc. Jpn. **87**, 033709 (2018).

[57] M. T. Suzuki, T. Nomoto, R. Arita, Y. Yanagi, S. Hayami, and H. Kusunose, Multipole expansion for magnetic structures: A generation scheme for a symmetry-adapted orthonormal basis set in the crystallographic point group, Phys. Rev. B **99**, 174407 (2019).